How Proteins Search for Their Specific Sites on DNA: The Role of DNA Conformation

Tao Hu,* A. Yu. Grosberg,* and B. I. Shklovskii*†
*Department of Physics, and †William I. Fine Theoretical Physics Institute, University of Minnesota, Minneapolis, Minnesota

ABSTRACT It is known since the early days of molecular biology that proteins locate their specific targets on DNA up to two orders-of-magnitude faster than the Smoluchowski three-dimensional diffusion rate. An accepted explanation of this fact is that proteins are nonspecifically adsorbed on DNA, and sliding along DNA provides for the faster one-dimensional search. Surprisingly, the role of DNA conformation was never considered in this context. In this article, we explicitly address the relative role of three-dimensional diffusion and one-dimensional sliding along coiled or globular DNA and the possibility of correlated readsorption of desorbed proteins. We have identified a wealth of new different scaling regimes. We also found the maximal possible acceleration of the reaction due to sliding. We found that the maximum on the rate-versus-ionic strength curve is asymmetric, and that sliding can lead not only to acceleration, but also in some regimes to dramatic deceleration of the reaction.

INTRODUCTION

The problem

Imagine that while you are reading these lines a λ-phage injects its DNA into *Escherichia coli* bacteria. For the infected cell, this sets a race against time: its hope to survive depends entirely on the ability of the proper restriction enzyme to find and recognize the specific site on viral DNA and then cut it, thus rendering viral DNA inoperable and harmless. If restriction enzyme takes too long to locate its target, then the cell is dead.

Restriction-modification system in bacteria, based on the endonuclease and methyltransferase enzymes, defends the prokaryotic cells against phage infection while also protecting the cell's own genome (1). This fact has already been recognized (2) as just one example of the molecular-biological system whose function hinges on the ability of certain proteins to locate their respective specific target sites on the DNA, and do that quickly. Another system on which fast protein-DNA recognition was studied quantitatively was *lac*-repressor, again in *E. coli*. This protein was found (3) to be able to locate its specific target on DNA up to two orders-of-magnitude faster than the so-called Smoluchowski limit, which corresponds to the search based solely on diffusion in three dimensions (4). This paradoxical result is sometimes referred to as faster-than-diffusion search.

As a matter of fact, the insufficiency of three-dimensional diffusion as a search mechanism in molecular biology was recognized even before any experiments, on purely theoretical grounds, by Delbrück (5), who also suggested resolving this problem by reducing the search dimension, i.e., by nonspecific adsorption on a one-dimensional macromolecule or two-dimensional membrane and then diffusing in this smaller space. Interestingly, as pointed out in the work (6), the idea that reduced dimension speeds up chemical reaction can be traced even further back to Langmuir, who noticed that adsorption of reagents on a two-dimensional surface can facilitate their diffusive finding each other (the ideas of Langmuir are nicely presented in (7)).

Capitalizing on the ideas of Delbrück, the authors Richter and Eigen (8) explained the *lac*-repressor experiment (3) by saying that three-dimensional diffusion has to bring protein into an elongated space region extended along DNA quite far from the specific target itself, where protein can nonspecifically adsorb on DNA and then slide along the DNA.

The field kept attracting intensive attention for many years. A nice recent review of various strategies employed to address the problem experimentally can be found in the work by Halford and Szczelkun (9). Based on the summary of experimental evidence, authors of this review conclude, that the process is not just a naive one-dimensional sliding, but rather a delicately weighted mixture of one-dimensional sliding over some distances and three-dimensional diffusion. This conclusion was further reiterated in the even more recent experimental work by Gowers et al. (10). A theorist also could have guessed the presence of a crossover between one-dimensional sliding and three-dimensional diffusion, because sliding along coiled DNA becomes very inefficient at large scale: having moved by $\sim t^{1/2}$ along DNA after one-dimensional diffusion over some time t, protein moves in space by only $t^{1/4}$ if DNA is a Gaussian coil. This is very slow subdiffusion. This is the situation requiring theoretical attention to how three-dimensional and one-dimensional diffusion can be combined, and how their combination should be manifested in experiments.

On the theoretical front, a major contribution to the field is due to Berg et al. (11). As an outcome of their theory, these authors formulated the following nice prediction, partially confirmed by their later in vitro experiments (12): the rate at

Submitted November 18, 2005, and accepted for publication January 12, 2006.

Address reprint requests to A. Yu. Grosberg, E-mail: grosberg@physics.umn.edu.

0006-3495/06/04/2731/14 $2.00 doi: 10.1529/biophysj.105.078162

which proteins find their specific target site on DNA depends in a nonmonotonic fashion on the ionic strength of the solution. In this context, ionic strength is believed to tune the strength of nonspecific adsorption of proteins on DNA, presumably because a protein adsorbs to DNA via positively charged patch on its surface. Thus, in essence one should speak of the nonmonotonous dependence of the rate on the energy of nonspecific adsorption of proteins on the DNA.

Although qualitatively consistent with experiment, the theory of Berg et al. (11) leaves several questions open. First and foremost, how does the search time of proteins finding their target, or the corresponding rate, depend upon the DNA conformation? In particular, is it important that the DNA is coiled at a length scale larger than the persistence length? Is it important that the DNA coil may not fit in the volume available, and then DNA must be a globule, like the nucleoid in a prokaryotic cell in vivo or under experimental conditions in vitro (13)? Second, a closely related aspect is that the theory of Berg et al. (11) does not answer the experimentally most relevant question (9) of the interplay between one-dimensional sliding and three-dimensional diffusion. In particular, one of the questions raised by experiments and not answered by the theory of Berg et al. (11) regards the correlations between the place where a protein departs from the DNA and the place where it readsorbs. The third aspect of the theory of Berg et al., although of a lesser importance and more dependent upon taste, is that it does not yield a simple intuitive explanation for nonmonotonic dependence of the rate on the strength of nonspecific adsorption. One may want to know whether a simple qualitative description of the rate exists, at least within some limits.

More recent refinement of the theory is given in Coppey et al. (14). The authors of this work follow Berg et al. in that they treat DNA in terms of domains—a concept having no unambiguous definition in the physics of DNA. Also, Coppey et al. (14) makes it very explicit that Berg et al. (11) and subsequent theories neglect correlations between the place where protein desorbs from DNA and the place where it adsorbs again—the approximation that clearly defies the polymeric nature and fractal properties of DNA. At the same time, this approximation leaves unanswered the experimentally motivated question of the interplay between one-dimensional and three-dimensional components of the search process.

In recent years, the problem was revisited by physicists several times (15–17), but the disturbing fact was that all of them attributed quite different results and statements to the findings of Berg et al. Bruinsma (15) says that according to Berg et al. (11), the search timescales as DNA lengths L rather than L^2, as in one-dimensional diffusion along DNA; Halford and Marko (16) state that proteins slide along DNA some distance—a distance that is independent of DNA conformation, regardless even of the DNA fractal properties. Slutsky and Mirny (17), however, concentrate on the role of the nonuniform DNA sequence, claiming that the time for three-dimensional diffusion must be approximately the same as the time for one-dimensional diffusion along DNA. A further, possibly even more disturbing fact is that none of these articles (11,14,15,17) make any clearly articulated explicit assumption about DNA conformation. Is it straight, or Gaussian coil with proper persistence length, or something else? Does the result depend on the DNA conformation? Interestingly, experimenters do discuss in their works (see (9) and references therein) the issue of correlated versus uncorrelated readsorption; these discussions call for theoretical attention and theoretical description in terms of correlations in fractal DNA, but so far, no proper theory has been suggested.

Motivated by these considerations, in this work we set out to reexamine the problem from the very beginning.

Model, approach, and limitations

We assume that within some volume υ, one (double-helical) DNA polymer is confined, with contour length L, persistence length p, and a target site of the size b.

Although in our theory we use a model of a single DNA molecule confined in the volume υ, all our results apply, without any modification, to a macroscopic solution of DNA, with concentration $1/\upsilon$ (in units of DNA chains per unit volume). For this solution, we assume that every DNA has to have contour length L and each DNA has to have one target site.

On a length scale smaller than that of the persistence length p, DNA is practically straight. In particular, if DNA contour length is shorter than p, i.e., $L < p$, DNA as a whole is rodlike. Long DNA, with $L > p$, coils up on the length scales exceeding p. We assume that the DNA coil is Gaussian, with overall size proportional to $R \sim (Lp)^{1/2}$ (as opposed to the swollen coil described by the Flory index 3/5 (18)). That means that we neglect the excluded volume effect. For DNA, this is a reasonable approximation for most realistic cases, such as, e.g., λ-DNA, because of the large persistence length/diameter ratio of the double helix: excluded volume in the coil remains unimportant (19) up to DNA length $\sim L < p^3/b^2$ (up to $\sim$100,000 basepairs under normal nonexotic ionic conditions).

We do allow for the possibility that the length of DNA L is so large that DNA Gaussian coil does not fit into the confinement volume υ, $R^3 > \upsilon$. In this case, DNA has to reflect many times back into the volume after touching the wall. We refer to this situation as DNA being a globule. We assume, however, that the volume fraction of DNA inside volume υ, which is $\sim Lb^2/\upsilon$, is sufficiently small even when DNA is a globule. In particular, we assume $Lb^2/\upsilon < b/p$, because in a denser system liquid crystalline nematic ordering of DNA segments becomes likely (19).

In terms of DNA solution, rodlike DNA (with $L < p$) and DNA coils are realized for the dilute solution, whereas a situation similar to that of the globule is realized for the semidilute solution (18) of DNA.

We further assume that protein can be nonspecifically adsorbed at any site on the DNA, and that nonspecific adsorption energy ϵ, or the corresponding constant $y = e^{\epsilon/k_BT}$, is the same everywhere on the DNA and does not depend on the DNA sequence. We also assume that every protein molecule has just one site capable of adsorbing to the DNA. (Although there are proteins with two such sites able to adsorb to two separate pieces of DNA at the same time and thus serve as a cross-linker for the DNA itself, we do not consider this possibility.)

We assume that nonspecifically bound protein can diffuse (slide) along DNA with the diffusion coefficient D_1, while protein dissolved in surrounding water diffuses in three dimensions with diffusion constant D_3. Thus, we have a unitless parameter related to the diffusion coefficients, $d = D_1/D_3$. In the simpler version of the theory (which we shall consider first), we assume $D_1 = D_3$, or $d = 1$. For simplicity, we assume that while protein is diffusing, either in three dimensions or along the DNA, the DNA itself remains immobile.

The quantity of our interest is the time needed for the target site to be found by a protein (consider, e.g., a restriction enzyme attacking a viral DNA intruder). One should imagine a certain concentration c of proteins randomly introduced into the system, and ask about the time needed for the first of these proteins to arrive at the target site. In this article, we will only address the mean time, averaged over both thermal noise and DNA conformation. For this averaged quantity, since the DNA is assumed immobile, the problem can be addressed in a simple way, by looking at the stationary rate. Namely, we should consider that there is a sink of proteins in the place of the specific target site, and that it consumes proteins with the rate J proportional to concentration c, which should be supported on a constant level by an influx to maintain stationarity. Obviously then, the averaged time is just $1/J$. At the end of the article, we show how to rederive all our results in terms of a single protein, thus avoiding an artificial assumption that there is a sink of proteins at the place of the target.

In this article, we calculate the rate J by assuming that concentration c is an arbitrary constant. To compare the predicted rate to the Smoluchowski rate $J_s = 4\pi D_3 cb$ (see Appendix A for a simple derivation of Smoluchowski formula), we shall mainly look at the ratio

$$\frac{J}{J_s} = \frac{J}{4\pi D_3 cb} \sim \frac{J}{D_3 cb}, \tag{1}$$

which characterizes the acceleration of the reaction rate achieved due to the sliding along the DNA.

We will be mainly interested in the scaling dependence of the rate J or acceleration J/J_s on major system parameters, such as y, L, and υ. In this context, we will use the symbol $\sim$ to mean *equal up to a numerical coefficient of order 1*, and the symbols $>$ and $<$ are to mean $\gg$ and $\ll$, respectively.

Along with dropping out all numerical coefficients in our scaling estimates, we also make several assumptions driven by a pure desire to simplify formulas and to clarify major physical ideas. We assume that all the microscopic length scales are of the same order, namely, approximately target size b: protein diameter, double-helical DNA diameter, and the distance from DNA at which nonspecific adsorption takes place. These assumptions are easy to relax, but in this article we shall touch neither of these issues, guided by the prejudice that simple questions should be addressed first.

The plan of the article is as follows. First, we consider the relatively simple cases when DNA is a Gaussian coil and one-dimensional sliding of proteins along DNA involves only a small part of DNA length. Already in this situation we will be able to explain the effect of correlated readsorption and arrive at a number of new results, such as, for instance, possible asymmetric character of the maximum on the curve of the rate as a function of adsorption strength. These results are also derived through the electrostatic analogy in the Appendix B. Second, we present a summary of all possible scaling regimes and then discuss them in more detail. We start this by looking at the rate saturation when one-dimensional sliding involves entire DNA length. Third, we consider a delicate case when DNA as a whole is a globule; in this case, we found that even the three-dimensional transport of proteins is in many cases realized through the sliding of adsorbed proteins along DNA and using DNA as a network of one-dimensional transport ways. We continue by looking at the situations when diffusion coefficient of the proteins along DNA is either smaller or larger than their diffusion coefficient in the surrounding bulk water. Fourth, we rederive all our major results using the language of single protein search time instead of a stationary process and flux. Finally, we conclude with comparison of our results to those of earlier works and the discussion of possible further implications of our work.

SIMPLE CASE: STRAIGHT ANTENNA VERSUS GAUSSIAN COIL ANTENNA

The reason why nonspecific adsorption on DNA can speed up the finding of the target is illustrated in Fig. 1, *a* and *b*: it is because DNA forms a kind of antenna around the target, thus increasing the size of the effective target. How should we determine the size of this antenna? The simplest argument is this. Suppose antenna size is ξ and contour length of DNA inside antenna is λ. It is worthwhile to emphasize that ξ and λ do not define any sharp border, but rather a smooth crossover, such that transport outside the antenna is mainly due to the three-dimensional diffusion, while transport inside the antenna is dominated by the sliding, or one-dimensional diffusion along DNA. The advantage of thinking about stationary process is that under stationary conditions, the flux of particles delivered by the three-dimensional diffusion into the ξ-sphere of antenna must be equal to the flux of particles

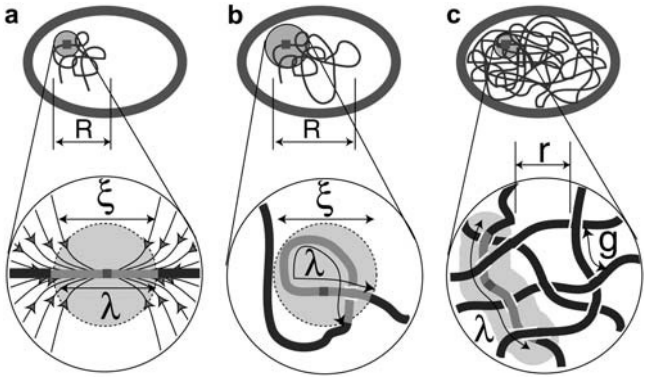

FIGURE 1 Antennae in a variety of cases. The upper part of every figure represents a poor man's idea of a prokaryotic cell. In panels *a* and *b*, DNA in the cell is a coil, because coil size R is smaller than the cell dimension; alternatively, one can think of a dilute solution of DNA in which R is much smaller than the distance to other coils (not shown). In panel *c*, the amount of DNA is so large that the coil size would have exceeded the cell diameter, and so DNA is a globule; alternatively, one can think of a semidilute solution (18) of strongly overlapping DNA coils. The lower figures represent a blown-up view of the region around the target site on DNA. The antenna part of DNA around the target is shown in lighter color than the rest of DNA. The space region below the crossover length scale is shadowed. This space region is roughly spherical in cases *a* and *b*; it is sausage-shaped in case *c*. Panel *a* also shows the averaged flow lines of the diffusion, which go in three dimensions far away from the target and go mostly along DNA within the antenna length scale (they are equivalent to electric field lines in terms of electrostatic analogy; see Appendix B). In panels *b* and *c*, flow lines are not shown, simply because it is difficult to draw them. In panel *c*, we see that DNA globule locally looks like a temporal network, with the mesh size r. In this case, the antenna might be much longer than one mesh. In the figure, the mesh size is not larger than the persistence length, so the length of DNA in the mesh g is approximately the same as r; at lesser density, mesh size might be longer, and then DNA in the mesh would be wiggly, with $g \gg r$.

delivered by one-dimensional diffusion into the target. The former rate is given by the Smoluchowski formula (see Appendix A) for the target size ξ; for the concentration of free (i.e., not adsorbed) proteins c_{free}, it is $\sim D_3 c_{\text{free}} \xi$. To estimate the latter rate, we note that the time of one-dimensional diffusion into the target site from a distance of order λ is $\sim \lambda^2/D_1$; therefore, the rate can be written as $(\lambda c_{\text{ads}})(\lambda^2/D_1)$, where λc_{ads} is the number of proteins nonspecifically adsorbed on the piece of DNA of the length λ. Thus, our main balance equation for the rate J reads

$$J \sim D_3 c_{\text{free}} \xi \sim \frac{D_1 c_{\text{ads}}}{\lambda}. \tag{2}$$

Formally, this equation follows from the continuity equation, which says that divergence of flux must vanish everywhere for the stationary process and that flux must be a potential field.

Notice that the balance equation, Eq. 2, depends on the relation between ξ and λ—between the size of antenna measured in space (ξ) and measured along the DNA (λ). Here, we already see why fractal properties of DNA conformations enter our problem.

To determine the one-dimensional concentration of nonspecifically adsorbed proteins, c_{ads}, and the concentration of proteins remaining free in solution, c_{free}, we now argue that as long as the antenna is only a small part of the DNA present, every protein in the system will adsorb and desorb many times on the DNA before it locates the target; therefore, there is statistical equilibrium between adsorbed and desorbed proteins. Assuming that we know the adsorption energy ϵ or the corresponding constant $y = e^{\epsilon/k_B T}$, and remembering that adsorbed proteins are confined within distance of order b from the DNA, we can write down the equilibrium condition as

$$c_{\text{ads}}/c_{\text{free}} b^2 = y, \tag{3}$$

which must be complemented by the particle-counting condition

$$c_{\text{ads}} L + c_{\text{free}}(\upsilon - Lb^2) = c\upsilon. \tag{4}$$

Since volume fraction of DNA is always small, $Lb^2 \ll \upsilon$, standard algebra then yields

$$\begin{aligned} c_{\text{ads}} &\simeq \frac{c\upsilon y b^2}{yLb^2 + \upsilon} \sim \begin{cases} cyb^2 & \text{if} \quad y < \upsilon/Lb^2 \\ c\upsilon/L & \text{if} \quad y > \upsilon/Lb^2, \end{cases} \\ c_{\text{free}} &\simeq \frac{c\upsilon}{yLb^2 + \upsilon} \sim \begin{cases} c & \text{if} \quad y < \upsilon/Lb^2 \\ c\upsilon/Lb^2 y & \text{if} \quad y > \upsilon/Lb^2. \end{cases} \end{aligned} \tag{5}$$

Note that at the length scales smaller than persistence length p, the DNA double helix is practically straight, while on the length scales greater than p, the double helix as a whole is a Gaussian coil. This means that, if we take a piece of double helix of the contour length λ, its size in space scales as

$$\xi \sim \begin{cases} \lambda & \text{when} \quad \lambda < p \\ \sqrt{\lambda p} & \text{when} \quad \lambda > p \end{cases}. \tag{6}$$

Substituting this result into the balance equation (Eq. 2), we can determine the antenna size and then, automatically, the rate—the latter being either side of the balance equation. We have to be careful, because we see that there are already as many as four different scaling regimes, due to Eqs. 5 and 6:

Regime A: Antenna is straight (upper expression of Eq. 6), adsorption is relatively weak (upper expressions in Eq. 5).

Regime B: Antenna is Gaussian (lower expression in Eq. 6), but adsorption is still relatively weak.

Regime C: Antenna is Gaussian and adsorption is relatively strong (lower expressions in Eq. 5).

Regime D: Straight antenna and strong adsorption.

Later we will find more regimes, but now let us consider just these four, one by one.

To begin with, suppose the antenna is straight ($\lambda < p$, so $\lambda \sim \xi$, see Fig. 1 *a*) and the nonspecific adsorption relatively weak ($y < \upsilon/Lb^2$, so $c_{\text{ads}} \sim cyb^2$). In this case, the balance equation yields $\lambda \sim b(yd)^{1/2}$, or the rate

$$J \sim c\sqrt{D_3 D_1}\, y^{1/2} b. \quad (7)$$

In other words, for the ratio of this rate to the Smoluchowski rate $J_s \sim D_3 cb$, we obtain

$$\frac{J}{J_s} \sim (yd)^{1/2} \quad \text{(regime A)}. \quad (8)$$

This result remains correct as long as antenna remains shorter than persistence length, and since we know λ, we obtain this condition explicitly: $y < p^2/b^2 d$.

Let us now suppose that nonspecific adsorption is still relatively weak ($y < \upsilon/Lb^2$, so $c_{ads} \sim cyb^2$), but it is strong enough such that the antenna is longer than persistence length ($\lambda > p$, so that $\xi \sim \sqrt{\lambda p}$, see Fig. 1 *b*). Then our balance equation yields $\lambda \sim (yd)^{2/3}\, p^{-1/3} b^{4/3}$ or

$$\frac{J}{J_s} \sim \left(\frac{ypd}{b}\right)^{1/3} \quad \text{(regime B)}. \quad (9)$$

One should check that this new result for λ implies that $\lambda > p$ at $y > p^2/b^2 d$, and so $y \sim p^2/b^2 d$ is the crossover line between the two regimes, *A* and *B*. In both regimes, and as expected, the rate grows with the strength of nonspecific adsorption, y, because increasing y increases the size of the antenna. However, the functional scaling dependence of the rate on y is significantly different, reflecting the difference in DNA fractality at different length scales.

Before we proceed with analysis of other scaling regimes, it is useful to make the following comment. The balance equation (Eq. 2) describes the fact that every protein going through the three-dimensional diffusion far away must then also go through the one-dimensional diffusion closer to the target. In other words, the balance equation (Eq. 2) describes the self-establishing match between the three-dimensional and one-dimensional parts of the process. But we can also look at the situation differently: suppose that one particular protein is adsorbed on DNA in a random place, and let us estimate the distance it can diffuse along DNA before it desorbs due to a thermal fluctuation. Since probability of thermally activated desorption is proportional to $e^{-\epsilon/k_B T} = 1/y$, the time that protein spends adsorbed must be $\sim b^2 y/D_3$. During this time, protein diffuses along DNA by the distance of $\sim\sqrt{D_1 b^2 y/D_3} = b\sqrt{yd}$. This distance was first estimated in Richter and Eigen (8); following Coppey et al. (14) and Halford and Marko (16), we call it sliding distance. We see, therefore, that antenna length λ is just about sliding distance for the straight DNA, but $\lambda \gg \ell_{slide}$ for the coiled DNA. At first glance, this seems like a very weird result: how can the antenna possibly be longer than the distance over which protein can slide? In fact, the antenna does become longer than the bare sliding distance, and this happens because, for the coiled DNA, every protein, desorbed after sliding the distance of the order of ℓ_{slide}, has a significant chance to readsorb nearby. Such correlated readsorption gets more likely as we consider more and more crumpled conformations of DNA. Indeed, if, in general, we assume that $\xi \sim \lambda^\nu$, then the balance equation yields $\lambda \sim y^{1/(1+\nu)}$, which means that λ grows with y faster than $\ell_{slide} \sim y^{1/2}$ at every $\nu < 1$. This growth of λ with y gets increasingly fast as ν decreases, which corresponds to more crumpled conformations. We should emphasize that this mechanism of correlated readsorption is impossible to see as long as polymeric and fractal properties of DNA are not considered explicitly, which is why this mechanism has been overlooked in previous works.

With further increase of either nonspecific adsorption strength y or DNA overall length L, we ran into the situation when most of the proteins are adsorbed on the DNA. In other words, if one prefers to think in terms of a single protein diffusion, then this single protein molecule spends most of the time adsorbed on DNA far away from the target. For this case, we have to use the lower lines of Eq. 5 and substitute it into the balance equation (Eq. 2). Since equilibrium condition, Eq. 3, is still satisfied, the result $\lambda\xi \sim ydb^2$ remains unchanged. Depending on whether antenna length λ is longer or shorter than persistence length, we obtain regimes *C* and *D*.

For regime *C*, we have $\lambda > p$; the antenna is a Gaussian coil; $\xi \sim \sqrt{\lambda p}$, yielding $\lambda \sim (yd)^{2/3} p^{-1/3} b^{4/3}$; and

$$\frac{J}{J_s} \sim \frac{\upsilon (pd)^{1/3}}{Lb^{7/3} y^{2/3}} \quad \text{(regime C)}. \quad (10)$$

Given our expression for λ, the condition $\lambda > p$ implies the familiar $y > p^2/b^2 d$, and another condition for this regime is that most proteins are adsorbed, or $y > \upsilon/Lb^2$ (see Eq. 5).

For regime *D*, the antenna is straight, so $\xi \sim \lambda$, and we get $\lambda \sim b(yd)^{1/2}$, just as in regime *A*. For the rate, however, substitution of the lower-line terms of Eq. 5 into the balance equation (Eq. 2) yields

$$\frac{J}{J_s} \sim \frac{\upsilon d^{1/2}}{Lb^2 y^{1/2}} \quad \text{(regime D)}. \quad (11)$$

According to our discussion, this regime should exist when $y < p^2/b^2 d$ and $y > \upsilon/Lb^2$. As we shall see later, these two conditions can be met together and the room for this regime exists only if $d < 1$, which means that one-dimensional diffusion along DNA is slower than three-dimensional diffusion in space.

In both regimes *C* and *D*, overall rate decreases with the increase of nonspecific adsorption, y, because three-dimensional transport to the antenna is slowed down by the lack of free proteins.

We have so far discussed four of the scaling regimes; our results are Eqs. 8–11. Already at this stage, we gained simple understanding of the nonmonotonic dependence of the rate on y—a phenomenon formally predicted in Berg et al. (11) and observed in Winter et al. (12), but previously not explained qualitatively: at the beginning, increasing y helps the process because it leads to increasing antenna length; further increase of y is detrimental for the rate because it leads to an unproductive adsorption of most of the proteins. We have also obtained a new feature, absent in previous

works: the shape of the maximum on the $J(y)$ curve is asymmetric, at least if DNA is not too long: in regimes B and C, rate grows as $y^{1/3}$ and then falls off as $y^{-2/3}$.

Since there are quite a few more scaling regimes, it is easier to understand them if we now pause to offer the summary of all regimes as presented in Fig. 2 and Table 1.

SUMMARY OF THE RESULTS: SCALING REGIMES

Our results are summarized in Fig. 2 and in the Table 1. Fig. 2 represents the log-log plane of parameters L and y, and each line on this plane marks a crossover between the scaling regimes. This figure gives the diagram of scaling regimes for the specific case $d = 1$ (or $D_1 = D_3$); later on, we will return to the more general situation and present corresponding diagrams for both $d < 1$ and $d > 1$ cases.

To be systematic, let us start our review of scaling regimes from the two trivial cases, which correspond to the axes in Fig. 2. When $y \leq 1$, there is no nonspecific binding of proteins to the DNA, and no sliding along the DNA. Proteins find their specific target at a rate equal to the Smoluchowski rate, or $J/J_s = 1$. Similarly, if the DNA is very short, as short as the specific target site itself, or $L \sim b$, then once again $J/J_s = 1$, for trivial reasons. Since we assume that there is some nonspecific adsorption, or $y \geq 1$, and since DNA length is obviously always greater than the target size b, our diagram in Fig. 2 presents only the $y > 1$ and $L/b > 1$ regions, which is why the pure Smoluchowski regime is seen only on the axes.

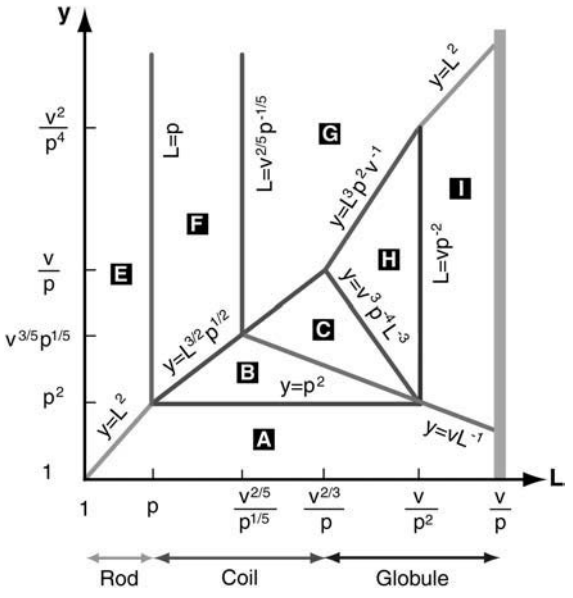

FIGURE 2 Diagram of scaling regimes for the case $d = 1$, when diffusion along the DNA has the same diffusion constant as diffusion in surrounding water. Both L and y axes are in the logarithmic scale. When DNA is shorter than the persistence length ($b < L < p$) it is essentially a rod, and if longer than the persistence length, is a Gaussian coil. However, coil size is smaller than the restriction volume υ ($p < L < \upsilon^{2/3}/p$), DNA is globular at $L > \upsilon^{2/3}/p$, and we only consider L up to $\sim\upsilon/pb$, because at larger L DNA, segments start forming a liquid-crystalline order. Summary of the rates for each regime is found in Table 1. Here, as well as in the other figures, to make formulas look shorter, all lengths are measured in the units of b, meaning that L, p, and υ stand for L/b, p/b, and υ/b^3.

If we increase y and consider the $y > 1$ situation, then we have significant nonspecific adsorption of proteins on DNA—which increases the rate due to the antenna effect. If y remains moderate, the antenna is shorter than DNA persistence length, and it is straight. This is the regime labeled A in Fig. 2 and described by Eq. 8. With further increase of y, when $y > p^2/b^2d$, we cross over into the regime labeled B and described by Eq. 9; in this regime, the antenna is so long that it is a Gaussian coil. From regime B, we can cross over the line $y = \upsilon/Lb^2$ and get into the regime labeled C and described by Eq. 10. One can cross over into regime C by either increasing y or increasing L, because increasing either of these variables promotes unproductive nonspecific adsorption of proteins on faraway pieces of DNA and thus slows down the transport to the specific target.

From regime A, we can also cross over the line $y = \upsilon/Lb^2$, but as long as $d = 1$, this does not bring us to regime D; instead, we get to the new regime labeled I, which we will explain below.

To understand all other scaling regimes, we have to remember that our previous consideration was restricted in two respects. First, we assumed that the entire DNA in the form of Gaussian coil fits within volume υ—which is true only as long as $L < \upsilon^{1/3}$ and $\sqrt{Lp} < \upsilon^{1/3}$, where $\upsilon^{1/3}$ stands for the linear dimension of the restriction volume. To relax this assumption, we will have to consider a long DNA, which is many times reflected by the walls of volume υ, and inside volume υ represents a globule, locally looking like a semidilute solution of separate DNA pieces, as illustrated in Fig. 1 *c*. For such long DNA, we shall find two more regimes, labeled H and I in Fig. 2. Second, we assumed that the antenna length λ was smaller than full DNA length L; the consequence of this was our statement, Eq. 3, that there is equilibrium between adsorbed and dissolved proteins. Relaxing this assumption, we will have to discuss regimes labeled E, F, and G in Fig. 2.

In Fig. 3, we present a schematic y-dependence of the rate for a number of values of DNA lengths L. Each curve is labeled with the corresponding value of L. To be specific, we have chosen the lengths that correspond to various crossovers and are marked on the scaling regimes diagram (Fig. 2). Note that in many cases our result for the rate exhibits a maximum and saturation beyond the maximum—features first described in Berg et al. (11). Unlike Berg et al., we find that the maximum is asymmetric and, even more importantly, J/J_s can become much smaller than unity, i.e., one can observe deceleration in comparison with Smoluchowski rate. We also find a number of other features, such as the specific power law scaling behavior of the rate.

Thus, we have to discuss one by one the new regimes E, F, G, H, and I. These will be addressed in the next section.

TABLE 1 The summary of rates and antenna lengths in various regimes

Regime	Description	J/J_s	λ
Axes	Smoluchowski: no antenna	1	b
A	Straight antenna, few proteins adsorbed	$(yd)^{1/2}$	$b(yd)^{1/2}$
B	Coiled antenna, few proteins adsorbed	$(ypd/b)^{1/3}$	$(yd)^{2/3}\ p^{-1/3}b^{4/3}$
C	Coiled antenna, most proteins adsorbed	$\upsilon(\mathrm{pd})^{1/3}/Lb^{7/3}\mathrm{y}^{2/3}$	$(yd)^{2/3}\ p^{-1/3}b^{4/3}$
D ($d < 1$)	Straight antenna, most proteins adsorbed	$\upsilon\mathrm{d}^{1/2}/Lb^{2}\mathrm{y}^{1/2}$	$b(yd)^{1/2}$
E	Whole DNA as straight antenna, few proteins adsorbed	L/b	L
F	Whole DNA as coiled antenna, few proteins adsorbed	$(Lp/b^2)^{1/2}$	L
G	Whole DNA as antenna, most proteins adsorbed	$\upsilon d/L^2 b$	L
H	Antenna with coiled mesh, most proteins adsorbed	$(p/b^2)(\upsilon d/Ly)^{1/2}$	$(b/p)(\upsilon yd/L)^{1/2}$
I	Antenna with straight mesh, most proteins adsorbed	$\upsilon\mathrm{d}^{1/2}/Lb^{2}\mathrm{y}^{1/2}$	$b(yd)^{1/2}$
K ($d > 1$)	Antenna with straight mesh, few proteins adsorbed	$(yd)^{1/2}$	$b(yd)^{1/2}$
M ($d > 1$)	Antenna with coiled mesh, few proteins adsorbed	$p(Lyd/\upsilon)^{1/2}$	$(b/p)(\upsilon yd/L)^{1/2}$

Note that, in labeling regimes, we skip J and L to avoid confusion with the rate and DNA length.

SYSTEMATIC CONSIDERATION OF SCALING REGIMES

DNA is not long enough for a full antenna

If DNA is too short for the antenna, then proteins already adsorbed on DNA can find their target faster than new proteins can be delivered to the DNA from solution. There is no longer any adsorption equilibrium, and instead of Eq. 3 we can only claim that $c_{\mathrm{ads}} < yc_{\mathrm{free}}b^2$. Therefore, the amount of adsorbed proteins under stationary conditions is physically determined by the stationarity itself, meaning that we have to look at Eq. 2 as two equations. In doing so, we have to replace λ in the right-hand side (one-dimensional rate) by L, because we do not have more DNA than L; and we have to replace ξ in the left-hand side, which is the antenna size for three-dimensional transport, by R, which is the overall size of the DNA coil. Of course, particle-counting Eq. 4 is still valid here, and it is the third equation. Thus, our equations read:

$$\frac{J}{J_s} \sim \frac{c_{\mathrm{free}}R}{cb};$$
$$c_{\mathrm{free}}R \sim \frac{c_{\mathrm{ads}}d}{L};$$
$$c_{\mathrm{ads}}L + c_{\mathrm{free}}\upsilon \sim c\upsilon. \tag{12}$$

From here, we find

$$\frac{J}{J_s} = \frac{\upsilon Rd/b}{RL^2 + \upsilon d}. \tag{13}$$

We can now easily address all possible scaling regimes in which the antenna is longer than the DNA.

To begin with, it is possible that DNA length is shorter than DNA persistence length $L < p$, such that the entire DNA is essentially straight, and then $R \simeq L$. Assuming also $L^3 < \upsilon$, we arrive at the scaling regime labeled E in Fig. 2, in this regime

$$\frac{J}{J_s} \sim \frac{L}{b} \quad (\text{regime E}). \tag{14}$$

The borderline of this regime can be established from the condition that since the entire DNA is smaller than the equilibrium antenna, we must expect that c_{ads} is smaller than its equilibrium value, or $c_{\mathrm{ads}}/c_{\mathrm{free}}b^2 \leq y$. Since, according to the second expression in Eq. 12 we have $c_{\mathrm{ads}}/c_{\mathrm{free}} = LR/d$, we then have the condition $LR/d < yb^2$; at $L < p$ this yields $y > L^2/b^2d$. At the same condition we can also arrive from the other side of the crossover, by noting that regime A continues as long as the antenna is shorter than the entire DNA, $\lambda < L$; and by using our result for λ for regime A, this produces the same crossover line between regimes A and E.

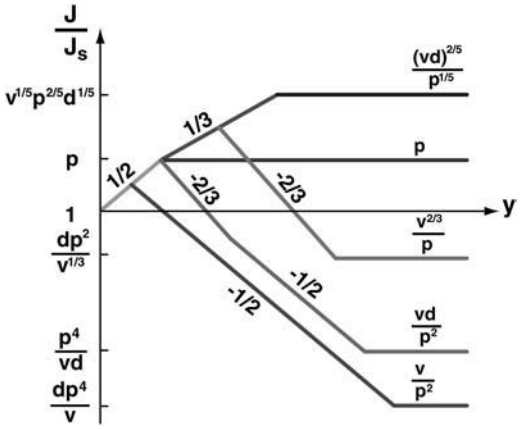

FIGURE 3 Schematic representation of rate dependence on y. Both the rate J and y are given in logarithmic scale. The fraction next to each curve shows its slope, which is the power of $J(y)$ dependence. Each curve corresponds to a specified value of DNA length. Also indicated in Fig. 2, the length is shown above the right end of each curve. Experimentally, the value of y can be controlled through the salt concentration, because nonspecific adsorption of proteins is controlled by Coulomb interaction between negative DNA and positive patch on the protein surface; for instance, if the salt is KCl, then it is believed (12,15) that $\lg y = 10 \lg [\mathrm{KCl}] + 2.5$, where [KCl] is the molar concentration of the salt. Note that we recover the possibility, first indicated in Berg et al. (11), that the rate goes through the maximum and then saturates; but in our case, the maximum is often asymmetric, and at large y the rate becomes very small $J/J_s \ll 1$, particularly for long DNA. Here, as well as in the other figures, to make formulas look shorter, all lengths are measured in the units of b, meaning that L, p, and υ stand for L/b, p/b, and υ/b^3.

For longer DNA, when $L > p$, the entire DNA is a Gaussian coil, and its size is $R \sim (Lp)^{1/2}$. Still assuming that the second term dominates in the denominator in Eq. 13, we arrive at

$$\frac{J}{J_s} \sim \left(\frac{Lp}{b^2}\right)^{1/2} \quad \text{(regime F)}. \tag{15}$$

This regime is labeled F in Fig. 2. Its border line with regime E is obviously the vertical line $L = p$. In regard to crossover to regime B, once again it can be established either from $c_{ads}/c_{free} = LR/d < y$ for regime F or from $\lambda < L$ for regime B. In either way, we arrive at the crossover condition $y = L^{3/2}p^{1/2}/b^2d$.

For even longer DNA, the antenna length becomes equal to the length of the entire DNA only at such large y that the system is already in regime C, with the rate falling down with increasing y because of the unproductive adsorption of proteins. Since antenna length λ in regime C is given by the same formula as in regime B, so the upper border line of regime C is the continuation of the corresponding line bordering regime B: $y = L^{3/2}p^{1/2}/b^2d$. However, when we cross this line upwards from regime C, we arrive at the new situation, because now the first term dominates in the denominator of the Eq. 13, meaning that most of the proteins are adsorbed on DNA, such that we obtain

$$\frac{J}{J_s} \sim \frac{\upsilon d}{L^2 b} \quad \text{(regime G)}. \tag{16}$$

The crossover between this regime and regime F is the vertical line at which both terms are comparable in the denominator of Eq. 13: $L = (\upsilon d)^{2/5}/p^{1/5}$. Crossover line with regime C can once again be established from the condition $c_{ads}/c_{free} = LR/d < y$.

In all regimes E, F, and G the rate saturates with increasing y. For regimes E and F this happens after just initial growth of the rate; for regime G, saturation occurs after the rate goes through the maximum and starts decreasing. In all cases saturation is due to the fact that increasing adsorption strength does not lead to any increase of the antenna size, because the entire DNA is already employed as antenna, and the antenna has nowhere to grow.

Cell is not big enough to house the DNA Gaussian coil

When DNA is very long for a given volume, that is, when $(Lp)^{1/2} > \upsilon^{1/3}$, DNA cannot remain just a coil; it must be a globule, as it is forced to return many times back into the volume after touching the walls (see, for example, (19)).

For the purposes of this work, it is sufficient to keep assuming that the excluded volume of DNA is not important, because the volume fraction of DNA within the confinement volume υ is still small, and is small even when compared at b/p. Nevertheless, locally the system looks like a so-called semidilute solution of DNA, or a transient network with a certain mesh size (see Fig. 1 *c*).

We should recall to mind some basic facts regarding the semidilute solution, or a transient network (18,19). Let us denote r as the characteristic length scale of a mesh in the network—which, in the scaling sense, is the same as the characteristic radius of density-density correlation (see Fig. 1 *c*). Let us further denote g as the characteristic length along the polymer corresponding to the spatial distance r. Quantities r and g can be estimated from the following physical argument (18,19): Consider a piece of polymer of the length g starting from some particular monomer; it occupies region $\sim r^3$ and makes density $\sim g/r^3$. This density must be approximately the overall average density, which for our system is of the order of L/υ. Thus, $g/r^3 \sim L/\upsilon$. The second relation between g and r is similar to Eq. 6, which depends upon whether the mesh size is bigger or smaller than persistence length p:

$$r \sim \begin{cases} g & \text{if} \quad g < p \\ \sqrt{gp} & \text{if} \quad g > p \end{cases}. \tag{17}$$

Accordingly, after some algebra, we obtain

$$\begin{aligned} &g \sim \sqrt{\frac{\upsilon}{L}}, \quad r \sim \sqrt{\frac{\upsilon}{L}} \quad \text{if} \quad L > \frac{\upsilon}{p^2} \\ &g \sim \frac{\upsilon^2}{L^2 p^3}, \quad r \sim \frac{\upsilon}{Lp} \quad \text{if} \quad \frac{\upsilon^{2/3}}{p} < L < \frac{\upsilon}{p^2}. \end{aligned} \tag{18}$$

The upper line of the expression above corresponds to a network so dense that every mesh is shorter than persistence length, and the polymer is essentially straight within each mesh. The lower line of the expression describes a much less concentrated network, in which every mesh is represented by a small Gaussian coil.

Returning to our problem, we should realize that the antenna length λ can in fact be longer than the mesh size g, as illustrated in Fig. 1 *c*. To estimate the antenna size for this case, we should remember that desorption from the antenna does not necessarily completely break the sliding along DNA, because protein can still readsorb on a nearby place on the DNA, or, more generally, on a correlated place on the DNA. To account for this, let us imagine that the antenna part of DNA is decorated by a tube of the radius r. Since r is the correlation length in the DNA solution, the protein remains correlated with the antenna as long as it remains within this tube around the antenna. Accordingly, our main balance equation, Eq. 2, must be modified to account for the fact that three-dimensional transport on scales larger than r is now realized through the DNA network and, therefore, the task of regular three-dimensional diffusion is only to deliver proteins over the length-scale of the order of one mesh size r, into any one of the λ/g network meshes along the antenna. The rate of delivery into one such mesh would be $\sim D_3 c_{free} r$, so that the overall delivery rate into the antenna tube scales as $\sim D_3 c_{free} r\lambda/g$. As usual, this must be equal to the rate of

one-dimensional delivery along the antenna into the specific target, so instead of Eq. 2 we finally get

$$J \sim D_3 c_{\text{free}} r \frac{\lambda}{g} \sim D_1 \frac{c_{\text{ads}}}{\lambda}. \quad (19)$$

As long as the antenna is shorter than the entire DNA, the relation between c_{free} and c_{ads} equilibrates and obeys Eqs. 3–5, so we finally get

$$\lambda^2 \sim b^2 \frac{gyd}{r} \quad (20)$$

and

$$\frac{J}{J_s} \sim \frac{c_{\text{free}}}{c} \frac{r\lambda}{g} \sim \frac{\upsilon}{Lb^2} \left(\frac{rd}{yg}\right)^{1/2}. \quad (21)$$

What is nice about this formula is that it remains correct in a variety of circumstances—when the antenna is straight ($\lambda < p$); or the antenna is Gaussian ($p < \lambda < \upsilon^{2/3}/p$); or the antenna is a globule ($\lambda > \upsilon^{2/3}/p$).

Taking r and g from Eq. 18, we finally obtain two new regimes. When every mesh is Gaussian,

$$\frac{J}{J_s} \sim \frac{p}{b^2} \left(\frac{\upsilon d}{Ly}\right)^{1/2} \quad (\text{regime H}). \quad (22)$$

This regime borders regime C along the line where the antenna size is equal to the mesh size, $\lambda = g$, which reads $y = \upsilon^3/(L^3 p^4 b^2 d)$. Regime H also borders regime G along the line where the antenna size is as long as the entire DNA, $\lambda = L$, or $y = L^3 p^2/\upsilon b^2 d$. Finally, regime H also borders another regime I along the vertical line $L = \upsilon/p^2$, which corresponds to the DNA within every mesh becoming straight (shorter than persistence length). For this regime, we have to use the upper line in the expressions in Eq. 18, thus obtaining

$$\frac{J}{J_s} \sim \frac{\upsilon d^{1/2}}{Lb^2 y^{1/2}} \quad (\text{regime I}). \quad (23)$$

This regime borders saturation regime G along the line $y = L^2/b^2 d$ where $\lambda = L$.

In regard to the lower border of regime I, it corresponds to the situation when the antenna becomes straight, which happens at $y = \upsilon/Lb^2 d$. However, as long as $d = 1$, which is the case presented in Fig. 2, this line coincides with the line $y = \upsilon/Lb^2$, below which most proteins are desorbed and free in solution. That is why at $d = 1$, there is no room for regime D, in which the antenna is straight, but most proteins adsorbed. Indeed, when $d = 1$, then three-dimensional transport is mostly realized by sliding along the network edges as soon as most proteins are adsorbed, which precisely means that regime A crosses over directly to regime I.

As we see, in both H and I regimes the rate J decreases with growing y, but does so more slowly than in regime C, that is, only as $y^{-1/2}$ instead of $y^{-2/3}$. This happens because adsorbed proteins are not just taken away from the process, as in regime C, but also participate in three-dimensional transport through the network (albeit this transport is still pretty slow).

This completes our scaling analysis for the $d = 1$ case shown in Fig. 2.

Diffusion rate along DNA is different from that in surrounding water

Let us now relax the $d = 1$ condition and examine the cases in which diffusion along the DNA is either slower ($d < 1$) or faster ($d > 1$) than in the surrounding water.

First, let us consider the $d < 1$ case, when diffusion along the DNA is slower than that in the surrounding water ($D_1 < D_3$); corresponding scaling regimes are summarized in the diagram Fig. 4 *a*. Most of the diagram is topologically similar to that in the Fig. 2, and we do not repeat the corresponding analysis. Of course, there are now powers of d in all equations, but the major qualitative novelty is that there is now room for regime D sandwiched between regimes A and I. The formal reason why this regime now exists in a separate region is because the line $y = \upsilon/Lb^2 d$ goes above the line $y = \upsilon/Lb^2$. To understand the more meaningful physical difference, let us recall that the line $y = \upsilon/Lb^2$ marks the crossover above which most of the proteins are adsorbed, but it is not enough for the sliding-along-network mechanism to dominate in the three-dimensional transport at $d < 1$.

Interestingly, the rate for both regimes D and I is given by the same formula (compare Eqs. 11 and 23). This happens because the antenna is straight for regime D and, while the antenna is not straight for regime I, it still consists of a number of essentially straight pieces, each representing one mesh. The major difference between regimes D and I, despite similar scaling of the rate, is in the mechanism of diffusion: in regime D, proteins diffuse through the water in a usual manner; whereas, in regime I, they are mostly transported along the network of DNA, with only short switches on the scale of one mesh size r between sliding tours. This is why straight pieces of DNA in different meshes independently add up to yield the same overall formula for the rate as in regime D.

Let us now switch to the opposite limit and consider the $d > 1$ case, for which the results are summarized in Fig. 4 *b*. This diagram is quite similar to the previously considered examples in Figs. 2 and 4 *a*, except there are now two new regimes labeled K and M (in alphabetical labeling of the regimes we skip J and L to avoid confusion with rate and DNA length). These regimes are both below the line $y = \upsilon/Lb^2$, which means that most of the proteins are not adsorbed. However, since $d > 1$, the new physical feature of the situation is that adsorbed proteins, although they are in minority, can nevertheless dominate in three-dimensional transport by sliding along the DNA network, because sliding is now so fast at $d > 1$. Thus, regimes K and M are ones in which effective diffusion along DNA network dominates, so we have to use Eq. 19 for the rate and antenna size, while for the

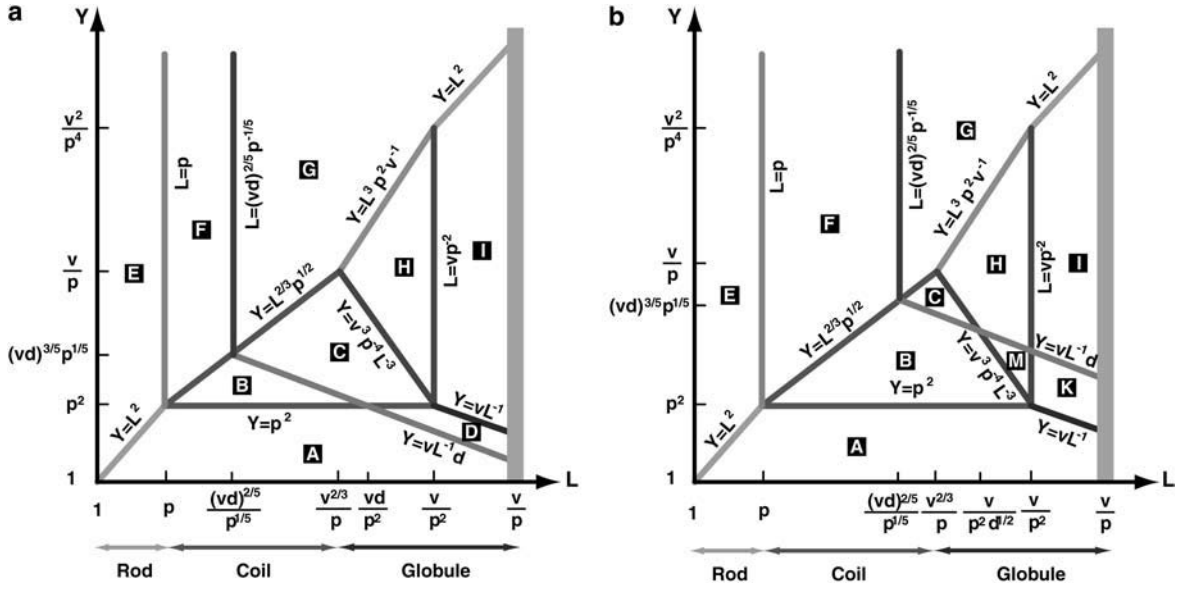

FIGURE 4 Scaling regimes for the cases $d < 1$ (*a*) and $d > 1$ (*b*). In this figure, $Y = yd$. Also, to make formulas look shorter, all lengths are measured in the units of b, meaning that L, p, and υ stand for L/b, p/b, and υ/b^3. The major difference from the $d = 1$ case is the presence of regime D in *a* and the presence of regimes K and M in *b*. In regime D, the majority of proteins are adsorbed, but the dominant three-dimensional transport is still the usual diffusion through the surrounding water, because sliding along the DNA is too slow ($D_1 < D_3$). In regimes K and M, the majority of proteins are not adsorbed, but the dominant three-dimensional transport mechanism is the sliding of minority proteins along the DNA network, because it is so much faster ($D_1 > D_3$). (Note that we skip J and L in labeling regimes to avoid confusion with rate J and DNA length L.)

concentrations of free and adsorbed proteins we have to use the upper line expressions in Eq. 5. In regime K, the local concentration of DNA segments is so high that every mesh in the DNA network contains an essentially straight piece of DNA, so we have to use the upper line expression in Eq. 18, yielding (after some algebra)

$$\frac{J}{J_s} \sim (yd)^{1/2} \quad (\text{regime K}). \tag{24}$$

Similarly, since in regime M, the mesh of the DNA network is Gaussian, we have to use the lower-line expression in Eq. 18, and this produces

$$\frac{J}{J_s} \sim p\left(\frac{Lyd}{\upsilon}\right)^{1/2} \quad (\text{regime M}). \tag{25}$$

Since the majority of proteins are not adsorbed, it is not surprising that the rate grows with y in both regimes K and M. Notice that the rate is given by the same formula as for regimes A and K (compare Eqs. 8 and 24). This is similar to the situation with regimes D and I, as discussed before, because even though the rate is given by the same formula, the underlying diffusion mechanism is fundamentally different. In both cases of D and I or A and K, it is possible that although scaling laws are the same, the numerical prefactors are different.

It is also interesting to note that the crossover between regimes B and M takes place on the line $y = \upsilon^3/p^4L^3b^2d$ where the antenna length is equal to the DNA length in one mesh: on the side of the B regime, the antenna is shorter than one mesh, and transport to the antenna must be through water; on the side of M, the antenna is longer than one mesh, and effective transport along the DNA network is at play.

Maximal rate

To finalize our discussion of scaling regimes, it is reasonable to ask: what is the maximal possible rate? According to our results, the maximal rate is achieved on the border between regimes F and G, that is, at $L \sim (\upsilon d)^{2/5}/p^{1/5}$ and at $y \geq \upsilon^{3/5}p^{1/5}/b^2d^{2/5}$. Maximal possible acceleration compared to the Smoluchowski rate is $\sim(\upsilon p^2 d/b^5)^{1/5}$. It is interesting to note that the optimal strategy in achieving the maximal rate at the minimal possible y requires us to have the adsorption strength y right at the level at which the probability of nonspecific adsorption for every protein is $\sim 1/2$ (on the line $y \sim \upsilon/Lb^2$).

It is interesting that the maximal possible acceleration grows with overall volume υ, which may seem counterintuitive. This result is due to the fact that total amount of DNA grows with increasing υ, and, according to our assumption, all this DNA has still just one target.

DISCUSSION

Single protein view

Many of the previous theoretical works (14–17) looked at the situation in terms of a single protein molecule diffusing to its

target. In this view, one should imagine that a protein molecule is initially introduced into a random place within volume υ, and then one should ask what is the first passage time (20) needed for the protein to arrive to the specific target site on DNA. The mean first-passage time τ can, of course, be found using our results for the rate J by inverting the value of the rate and assuming that, on average, there is just one protein molecule in the system at any time, i.e., $\tau = 1/J|_{c=1/\upsilon}$. However, we want to rederive all our results directly in terms of τ to build bridges to the works of other authors. The rederivation also turns out quite illuminating.

First let us consider that DNA is a globule, $L > \upsilon^{2/3}/p$ (or semidilute solution), and look at regimes H, I, K, and M; unlike stationary diffusion approach above, in the single protein language the derivation for the globular DNA case is actually simpler. Following Slutsky and Mirny (17), we imagine that the search process for the given single protein consists of tours of one-dimensional sliding along DNA followed by diffusion in three-dimensions, followed by one-dimensional sliding, etc. If in one tour of one-dimensional sliding, protein moves some distance λ along the DNA, then it takes time at $\sim\lambda^2/D_1$. The length λ here is, of course, our familiar antenna length, but we will rederive it here, so we do not assume it known. In regard to the tour of three-dimensional diffusion, it breaks the correlation of the one-dimensional sliding if it carries the protein over a distance larger or approximately the same as the correlation length in the DNA system, which is r—mesh (or blob) size. Thus, the longevity of one tour of three-dimensional diffusion is $\sim r^2/D_3$.

The next step of our argument is this. On its way to the target, the protein will go through a great many adsorption and desorption cycles; therefore, the ratio of time that protein spends adsorbed and desorbed should simply follow equilibrium Boltzmann statistics:

$$\frac{\lambda^2/D_1}{r^2/D_3} \sim \frac{yLb^2}{\upsilon}. \tag{26}$$

Here, we note that there is an approximation underlying our argument: one tour of correlated one-dimensional sliding does include small three-dimensional excursions of the protein into water, but they are small in the sense that they do not go beyond the crossover correlation distance and, therefore, readsorption after excursion occurs at a correlated place on the DNA. Accordingly, these excursions make only a marginal contribution to the sliding time, which is correctly estimated as $\sim\lambda^2/D_1$.

The final part of the argument is most clearly formulated by Bruinsma (15): since subsequent tours of one-dimensional sliding occur over uncorrelated parts of DNA, full search requires $\sim L/\lambda$ rounds. Therefore, the total search time τ can be written as

$$\tau \sim \frac{L}{\lambda}\left[\frac{\lambda^2}{D_1} + \frac{r^2}{D_3}\right]. \tag{27}$$

Equations 26 and 27 solve the problem for all regimes of globular DNA if we remember that mesh (or blob) size r is given by Eq. 18. Notice that Eq. 26 gives a new interpretation to the line $y \sim \upsilon/Lb^2$ on any of our diagrams in Fig. 2 and Fig. 4, *a* and *b*: for the parameters below this line most of the overall search time is spent in three-dimensional diffusion, while for the system with parameters above the line the major time-consuming part is the one-dimensional sliding. It is close to this line where the result of Slutsky and Mirny (17) applies and these two times are of the same order. And let us recall that it is also close to this line where the maximal possible rate is achieved (see Maximal Rate, above).

Thus, regimes H, I, K, and M result from two possibilities for r in Eq. 18 (straight or Gaussian DNA within a mesh) and two possibilities of either first- or second-term dominance in Eq. 27.

Let us now turn to regimes A, B, C, and D, in which DNA is a coil. In this case, we still essentially rely on the equations similar to Eqs. 26 and 27, except some effort is now needed to understand the time of three-dimensional diffusion.

Our argument for this case starts from our noticing that there is a crossover spatial scale ξ, such that correlated sliding takes place inside scale ξ, while regular three-dimensional diffusion in water occurs on a larger length scale, as it breaks correlations between desorption and subsequent readsorption. Thus, the time of one tour of three-dimensional diffusion is the mean first-passage time into any one of the L/λ spheres of size ξ (here λ is the contour length of DNA accommodated by one sphere of the size ξ; once again, we pretend that we do not know ξ and λ, but will rederive them in this single-protein language). The arrival time into one such sphere is the Smoluchowski time (discussed in Appendix A) for the target of size ξ, which is $\sim\upsilon/D_3\xi$; the arrival time into any one of the L/λ spheres is L/λ times smaller, $\sim\upsilon/D_3\xi(L/\lambda)$ To present our equations for λ and overall search time τ in form similar to Eqs. 26 and 27, we define distance r_{eff} such that $r_{\text{eff}}^2 \sim D_3[\upsilon/D_3\xi(L/\lambda)] = \upsilon\lambda/L\xi$, and then we obtain

$$\frac{\lambda^2/D_1}{r_{\text{eff}}^2/D_3} \sim \frac{yLb^2}{\upsilon} \tag{28}$$

and

$$\tau \sim \frac{L}{\lambda}\left[\frac{\lambda^2}{D_1} + \frac{r_{\text{eff}}^2}{D_3}\right]. \tag{29}$$

Once again, remembering two regimes for the relation between λ and ξ, Eq. 6, and having either the first or second term dominate in the total time of Eq. 29, we recover the regimes A, B, C, and D.

Finally, the results for all saturation regimes E, F, and G are recovered by replacing the antenna length λ with L in Eqs. 27 or 29, and replacing equality with inequality in the conditions of Eqs. 26 or 28.

Comparison with earlier theoretical works

Let us now compare our findings with various statements found in the literature. The most widely known result of Berg et al. (11) was the prediction, later confirmed experimentally (12), that the rate depends on y (controlled by ionic strength) in a characteristic way, exhibiting a maximum followed by a plateau. We have recovered this as a possible scenario for some combinations of parameters (regimes), as shown in Fig. 3. However, we also found a number of additional features not noticed previously: first, the maximum is in many cases asymmetric; second, the scaling of rate dependence on y exhibits rich behavior, with the possibilities of crossing over from $y^{1/2}$ to $y^{1/3}$ on the way to the maximum, or from $y^{-2/3}$ to $y^{-1/2}$ on the way down; third, there is a possibility of very strong deceleration at large adsorption strength y compared at the Smoluchowski rate. All of these features have a simple qualitative explanation: the rate grows because increasing y increases the antenna; the rate decays when most of the proteins are fruitlessly adsorbed far from the target (or, in other words, every protein spends most of the time adsorbed far away); and the rate saturates and comes to the plateau because the antenna becomes as long as the DNA itself. All of these features are the direct consequence of the fractal properties of DNA, in either a coil or globule state.

Bruinsma (15) presents a review of a variety of topics related to protein-DNA interactions, and the issue of the search rate is considered only briefly. In that context, Bruinsma (15) provides an important insight, used above in presenting Eq. 27, that subsequent rounds of one-dimensional search are performed on uncorrelated pieces of DNA. In other words, there exists a crossover from mostly correlated events (earlier combined into one correlated sliding length λ) to mostly *un*correlated events. In accord with this insight, the search time is linear in DNA length only in regime *I*.

In the work by Halford and Marko (16), the antenna length was explicitly identified with the sliding distance (that is, with the bare sliding distance, earlier in this article denoted $\ell_{\text{slide}} \sim b\sqrt{yd}$), and then essentially Eq. 27 was used to determine the search time. This approach is perfectly valid only as long as the antenna is straight, $\lambda = \xi$, and $\lambda = \ell_{\text{slide}}$ (which predicts the symmetric maximum of $J(y)$ dependence), but it should not be used when the DNA antenna is coiled. For the globular DNA, the approximation of the straight antenna—implicit in the identification of λ with bare ℓ_{slide}—is valid for the right end of regime *A* and for regime *D*, although, of course, other globular regimes require going beyond this approximation.

The main emphasis of Slutsky and Mirny (17) is on the role of nonuniform sequence of DNA, which may lead to nonspecific adsorption strength y, or to one-dimensional diffusion coefficient D_1, or for both to be noisy functions of coordinate on DNA. In their review of the uniform homopolymer case, Slutsky and Mirny (17) employ formulas equivalent to our Eqs. 27 or 29, but instead of conditions as in Eqs. 26 or 28, they minimize overall time with respect to λ. As we pointed out before, this approach is only valid within the crossover corridor around the line $y \sim \upsilon/Lb^2$. In general, the idea of applying a variational principle is very interesting. It can be generalized beyond the above mentioned corridor if one minimizes the overall dissipation, which is equivalent to energy minimization in terms of electrostatic analogy, as we show in Appendix B. Of course, minimization of dissipation is equivalent to the diffusion equation as long as diffusion is linear in gradients. Alternatively, one can also think, as emphasized in Halford and Marko (16), that search mechanism was subject to optimization by biological evolution. To employ this idea, it is obviously necessary first to understand the possible search scenario, or regimes, existing in physics, and then, in the next stage, one could attempt optimization with respect to the parameters, such as DNA packing properties, etc., which could be subject to selective pressure in evolution.

Berg et al. (11) and some subsequent authors treated the DNA solution in terms of domains. Although this domains-term was never very clearly defined, it could be understood as space regions more or less occupied by separate DNA coils in solution. With such an understanding, the terminology of domains can be used as long as the DNA coil fits into the volume υ; or, in other words, is best suitable for an in vitro experiment in which DNA solution is dilute, such that DNA coils do not overlap. The terminology of DNA domains becomes unsatisfactory at larger DNA concentrations.

Coppey et al. (14) considered the stochastic approach, which means they did not look at the stationary diffusion, but rather at the trajectory of a single protein. As we pointed out before, these approaches must be equivalent as long as one is only interested in the average time of the arrival of the first proteins. The important contribution of Coppey et al. (14) was the elucidation of the crucial neglect of the correlations between the desorption point of a protein and its readsorption point. It is because of this crucial and not always justified approximation that previous theories appear to have overlooked the mechanism of correlated readsorption, which is entirely due to the DNA being a polymer and a fractal coil. Correlated readsorption was anticipated by Halford and Szczelkun (9).

Experimental situation

Most of the experiments in the field (see (9) and references therein) involve various ingenious arrangements of two or more target sites on the linear or ring DNA and observation of the resulting enzyme processivity. In the light of our theory, it would be interesting to revive the earlier Berg et al.-style experiments and to look carefully at the theoretically predicted multiple features of $J(y)$ curves, such as asymmetric maximum, various scaling regions, the possible deceleration, and so forth.

The seeming difficulty is that all our interesting regimes start when $y > p^2/b^2d$, when the antenna is longer than the DNA persistence length. Since the persistence length of dsDNA, p, is fairly large, ~150 basepairs under usual ionic conditions (say, [Na] = 0.2 M), and assuming b is approximately the diameter of the double helix, we get $p/b \approx 25$ for the dsDNA. Unless d is large, this seems to require nonspecific adsorption energies, ~6–10 k_BT, which is high but not impossible. In any case, we would like to emphasize that the maximum $J(y)$ has been observed (12), which, according to our theory, could have happened only at $y > p^2/b^2d$, thus assuring that this range is within reach.

One of the most critical and poorly known parameters of our theory is $d = D_1/D_3$. Of course, D_3 (diffusion coefficient of the protein in water), is rather well known, and this can be simply estimated based on its size using the Stokes-Einstein relation. The difficult part is about D_1, which involves friction of the protein against DNA in the solvent. It is clear that slow diffusion along DNA would make the entire mechanism of one-dimensional sliding less efficient, and indeed decreasing d systematically reduces the rate that we obtain in almost all regimes. There are only two exceptions to this: one is trivial—a pure Smoluchowski process not involving any sliding, and realized only when there is no nonspecific adsorption on DNA ($y \leq 1$). The other is in regimes E and F, regimes when the entire DNA, rodlike or coil-like, serves as an antenna, which means three-dimensional transport to the DNA is the slowest part, the bottleneck of the whole process, so that reducing d does not do any damage—except, of course, in pushing away the corresponding regime boundaries.

Experimental data on the one-dimensional diffusion of proteins along DNA are scarce and not completely clear (21). Very recently, when our work was already written down, the new article of Wang et al. (22) became available, in which the authors report application of modern single molecule techniques to measure D_1.

Finally, we comment on the state of DNA to be used in experiment. In our theory, we dealt with the model of a single DNA confined in some volume υ. This is reminiscent of the DNA in vivo, confined in a prokaryotic cell. Of course, a real nucleoid is a rather complex structure involving far more sophisticated features than just overall compaction; they are caused by structural and other proteins, by entanglements, etc. (see (13) and references therein). The cases of rodlike DNA ($L < p$) or coil-like DNA ($p < L < \upsilon^{2/3}/p$) can be adequately modeled by an in vitro experiment involving a dilute solution of DNA, with $1/\upsilon$ DNA chains per unit volume. Since the DNA coil is typically much larger than the prokaryotic cell, our results for the compacted, or globular, DNA are relevant. The question of an adequate in vitro model of such DNA conformations is quite delicate (23,24), and goes beyond the scope of this work; we note, however, that our present theory can be tested simply by considering the semidilute solution of DNA chains.

CONCLUSION

Many questions remain open. The role of concurrent protein species, the role of nonuniform DNA sequence, the role of DNA motion (25), the probability of unusually long search times, the search on a single-stranded DNA or RNA, the role of superhelical structures, the dependence of rate (or search time) on the specific positions of one or more targets on DNA, the related issue of enzyme processivity, the role of excluded volume for very long DNA and corresponding loop-erasing walks (26)—all of these questions invite theoretical work.

To conclude, we have analyzed all scaling regimes of the diffusion-controlled search by proteins of the specific target site located on DNA. We found many regimes. The major idea can be formulated in terms of the crossover between one-dimensional sliding along DNA up to a certain length scale and three-dimensional diffusion in surrounding space on the larger length scale. Overall, qualitatively, this idea seems to be in agreement with the intuition expressed in experimental articles. In addition, we have made several theoretical predictions which are verifiable and (even more importantly) falsifiable by the experiments. We are looking forward to such experiments.

APPENDIX A: SIMPLE SCALING DERIVATION OF THE SMOLUCHOWSKI RATE AND THE SMOLUCHOWSKI TIME

Classical Smoluchowski theory (4) treats the diffusion-controlled process of irreversible absorption of diffusing particles by an immobile sphere of a given radius; call it b. As in our proteins problem, Smoluchowski theory can be formulated either in terms of stationary rate, J_s, assuming concentration c is fixed; or in terms of mean first-passage time, τ_s, for a single protein.

Let us imagine that a protein diffuses within a volume υ, and its diffusion coefficient is D_3. Let us further define the time interval t_b such that, over time t_b, the protein moves the distance of order b, which is $D_3 t_b \sim b^2$. Then, over a longer time t, the protein visits t/t_b spots of size b each, and, given that $b_3 \ll \upsilon$, the probability that none of these spots are the target, or the probability to keep missing the target for the time t obeys Poisson distribution and decays exponentially with t, is $(1 - b^3/\upsilon)^{t/t_b} \simeq \exp[-tb^3/(\upsilon t_b)]$. The mean first-passage time is read out of the formula $\tau_s \sim \upsilon/(D_3 b)$.

The corresponding stationary rate is obtained by inverting this time, assuming overall concentration of proteins, $c = 1/\upsilon$. Thus, $J_s \sim D_3 cb$.

Of course, more accurate derivation, available in a number of textbooks (and easily formulated in terms of electrostatic analogy, see Appendix B), is necessary to complement the result with the correct prefactor of 4π.

APPENDIX B: ELECTROSTATIC ANALOGY

Here, we rederive the results of the section regarding simple cases using the fact that the stationary diffusion equation is the same as the Laplace equation in electrostatics. Specifically, the problem of diffusion into the target of the size b is equivalent to the problem of finding the electric field around a charge of the size b. The key relatively nontrivial point of this analogy is to realize that the potential well for diffusing particles is equivalent, in electrostatic language, to the region in space with a very high dielectric constant. In our case, the potential well is located all around DNA, and

the target is also somewhere on the DNA. Therefore, it is equivalent to the electrostatic problem in which we have a channel, of the diameter $\sim b$, filled with a high dielectric constant material such as water, surrounded by a low dielectric constant material. Specifically, it is easy to check that y of the diffusion problem is exactly equivalent to ϵ_w/ϵ_m; the ratio of dielectric constants of water and surrounding medium, $y = \epsilon_w/\epsilon_m \gg 1$.

Thus, we have to address the problem of a charge Q located inside the water-filled channel in, for example, a thick lipid membrane. For the straight channel, this is a well-known problem in membrane biophysics. It was first studied by Parsegian (27), and the recent most detailed exposition is given in Kamenev et al. (28) (see also (29,30)). Here, we give only simple scaling consideration.

Since $\epsilon_w/\epsilon_m \gg 1$, field lines prefer to remain inside the channel for as long as possible. This gives the picture of the electric field equivalent to the Fig. 1, *a*. In other words, we should say that there is some length scale λ along the channel, and within this scale, electric field lines are predominantly confined in the channel. At the same time, outside of the sphere of radius ξ, the electric field is close to that of a spherical charge in unrestricted space. Thus, electric field energy can be approximated as the sum of two parts, one due to the uniform field in the volume at $\sim b^2\lambda$ in the channel, and the other around the ξ-sphere in the medium. Since the E-field in the channel is $\sim Q/b^2\epsilon_w$ and D-field is Q/b^2, the energy due to the field inside the channel is $\sim(Q/b^2\epsilon_w)\times(Q/b^2)\times(b^2\lambda) = Q^2\lambda/b^2\epsilon_w$. At the same time, energy of the field in the outer zone is $\sim Q^2/\xi\epsilon_m$. Thus, total electrostatic energy (self-energy of the charge Q) is

$$E \sim \frac{Q^2\lambda}{b^2\epsilon_w} + \frac{Q^2}{\xi\epsilon_m}. \tag{30}$$

To begin with, let us assume that the channel is straight. Then, $\lambda = \xi$, and minimization of the energy formula in Eq. 30 gives $\lambda \sim b\sqrt{\epsilon_w/\epsilon_m} \gg b$. This formula was derived by Finkelstein and Ptitsyn (31). Given that $y = \epsilon_w/\epsilon_m$, this formula (Eq. 30) is equivalent to our result for the antenna length in the straight antenna regime A (assuming $d = 1$).

Consider now the coiled channel; such a problem was never considered in electrostatic context, but one can imagine, for instance, a flexible fiber of high dielectric constant material surrounded by air. Equation 30 still applies, but $\xi \sim \sqrt{\lambda p}$. Minimization then yields $\lambda \sim b^{4/3}p^{-1/3}(\epsilon_w/\epsilon_m)^{2/3} = b^{4/3}p^{-1/3}y^{2/3}$, which is our result for the antenna length in regime B.

To conclude, we note that minimization of energy in the electrostatic language is translated to minimization of dissipation in the diffusion language.

We gratefully acknowledge very useful discussions with J.-L. Sikorav. We also thank M. Frank-Kamenetskii for advice, and R. Austin for sending us a preprint of Wang et al. (22) before its publication.

The work of A.Y.G. was supported in part by the Materials Research Science and Engineering Center Program of the National Science Foundation under Award No. DMR-0212302.

REFERENCES

1. Gormley, N. A., M. A. Watson, and S. E. Halford. 2001. Bacterial-Restriction Modification Systems. Encyclopedia of Life Sciences. http://www.els.net/. Nature Publishing Group.
2. Arber, W. 1971. The Bacteriophage Lambda. A. D. Hershey, editor. Cold Spring Harbor Laboratory, Cold Spring Harbor, NY. 83–96.
3. Riggs, A. D., S. Bourgeois, and M. Cohn. 1970. The *lac* repressor-operator interaction. III. Kinetic studies. *J. Mol. Biol.* 53:401–417.
4. Smoluchowski, M. V. 1917. Attempt of mathematical theory of coagulation kinetics in colloidal solutions. *Z. Phys. Chem.* 92:129–198.
5. Adam, G., and M. Delbrück. 1968. Structural Chemistry and Molecular Biology. A. Rich, and N. Davidson, editors. W. H. Freeman, San Francisco, CA. 198–215.
6. Goldar, A., and J.-L. Sikorav. 2004. DNA renaturation at the water-phenol interface. *Eur. Phys. J. E.* 14:211–239.
7. Zangwill, A. 1988. Physics at Surfaces. Cambridge University Press, Cambridge, UK.
8. Richter, P. H., and M. Eigen. 1974. Diffusion controlled reaction rates in spheroidal geometry. Application to repressor-operator association and membrane bound enzymes. *Biophys. Chem.* 2:255–263.
9. Halford, S. E., and M. D. Szczelkun. 2002. How to get from A to B: strategies for analysing protein motion on DNA. *Eur. Biophys. J.* 31: 257–267.
10. Gowers, D. M., G. G. Wilson, and S. E. Halford. 2005. Measurement of the contributions of one-dimensional and three-dimensional pathways to the translocation of a protein along DNA. *Proc. Natl. Acad. Sci. USA.* 102:15883–15888.
11. Berg, O. G., R. B. Winter, and P. H. von Hippel. 1981. Diffusion-driven mechanisms of protein translocation on nucleic acids. 1. Models and theory. *Biochemistry.* 20:6929–6948.
12. Winter, R. B., O. G. Berg, and P. H. von Hippel. 1981. Diffusion-driven mechanisms of protein translocation on nucleic acids. 3. The *Escherichia coli lac* repressor-operator interaction: kinetic measurements and conclusions. *Biochemistry.* 20:6961–6977.
13. Cunha, S., C. L. Woldringh, and T. Odijk. 2005. Restricted diffusion of DNA segments within the isolated *Escherichia coli* nucleoid. *J. Struct. Biol.* 150:226–232.
14. Coppey, M., O. Benichou, R. Voituriez and M. Moreau. 2004. Kinetics of target site localization of a protein on DNA: a stochastic approach. *Biophys. J.* 87:1640–1649.
15. Bruinsma, R. F. 2002. Physics of protein-DNA interaction. *Physica A.* 313:211–237.
16. Halford, S. E., and J. F. Marko. 2004. How do site-specific DNA-binding proteins find their targets? *Nucleic Acids Res.* 32:3040–3052.
17. Slutsky, M., and L. A. Mirny. 2004. Kinetics of protein-DNA interaction: facilitated target location in sequence-dependent potential. *Biophys. J.* 87:4021–4035.
18. deGennes, P. G. 1979. Scaling Concepts in Polymer Physics. Cornell University Press, Ithaca, NY.
19. Grosberg, A. Y., and A. Khoklov. 1994. Statistical Physics of Macromolecules. AIP Press, New York, NY.
20. Redner, S. 2001. A Guide to First Passage Processes. Cambridge University Press, Cambridge, UK.
21. Ehbrecht, H.-J., A. Pingoud, C. Urbanke, G. Maass, and C. Gualerzi. 1985. Linear diffusion of restriction endonucleases on DNA. *J. Biol. Chem.* 260:6160–6166.
22. Wang, Y. M., R. H. Austin, and E. C. Cox. 2005. Single molecule measurements of repressor protein 1-D diffusion on DNA. preprint.
23. Sikorav, J.-L., and G. M. Church. 1991. Complementary recognition in condensed DNA: accelerated DNA renaturation. *J. Mol. Biol.* 222: 1085–1108.
24. Jary, D., and J.-L. Sikorav. 1999. Cyclization of globular DNA. Implications for DNA-DNA interactions in vivo. *Biochemistry.* 38:3223–3227.
25. von Hippel, P. H., and O. G. Berg. 1989. Facilitated target location in biological systems. *J. Biol. Chem.* 264:675–678.
26. Lawler, G. F. 1987. Loop-erased self-avoiding random walk and the Laplacian random walk. *J. Phys. A Math. G E N.* 20:4565–4568.
27. Parsegian, A. 1969. Energy of an ion crossing of a low dielectric membrane: solutions to four relevant electrostatic problems. *Nature.* 221:844–846.
28. Kamenev, A., J. Zhang, A. I. Larkin, and B. I. Shklovskii. 2006. Transport in 1D Coulomb gases: from ion channels to nanopores. *Physica A.* 359:129–161.
29. Jordan, P. C. 1982. Electrostatic modeling of ion pores. Energy barriers and electric field profiles. *Biophys. J.* 39:157–164.
30. Teber, S. 2005. Translocation energy of ions in nano-channels of cell membranes. Cond-mat/0501662.
31. Finkelstein, A. V., and O. B. Ptitsyn. 2003. Protein Physics: A Course of Lectures. Academic Press, San Diego, CA.